PASSAGE OF PARTICLES THROUGH MATTER

To reduce the size of this section's PostScript file, we have divided it into three PostScript files. We present the following index:

PART 1

PART 2

PART 3

23. PASSAGE OF PARTICLES THROUGH MATTER

Revised May 1998 by D.E. Groom (LBNL).

23.1. Notation

Table 23.1: Summary of variables used in this section. The kinematic variables β and γ have their usual meanings.

Symbol	Definition	Units or Value
α	Fine structure constant	$1/137.035\,989\,5(61)$
M	Incident particle mass	MeV/c^2
E	Incident particle energy γMc^2	MeV
T	Kinetic energy	MeV
$m_e c^2$	Electron mass $\times\ c^2$	$0.510\,999\,06(15)$ MeV
r_e	Classical electron radius $e^2/4\pi\epsilon_0 m_e c^2$	$2.817\,940\,92(38)$ fm
N_A	Avogadro's number	$6.022\,136\,7(36) \times 10^{23}$ mol^{-1}
ze	Charge of incident particle	
Z	Atomic number of medium	
A	Atomic mass of medium	g mol^{-1}
K/A	$4\pi N_A r_e^2 m_e c^2/A$	0.307 075 MeV g^{-1} cm^2 for $A = 1$ g mol^{-1}
I	Mean excitation energy	eV
δ	Density effect correction to ionization energy loss	
$\hbar\omega_p$	Plasma energy $\sqrt{4\pi N_e r_e^3}\ m_e c^2/\alpha$	$28.816\sqrt{\rho\langle Z/A\rangle}$ eV[a]
N_c	Electron density	(units of r_e)$^{-3}$
w_j	Weight fraction of the jth element in a compound or mixture	
n_j	$\propto$ number of jth kind of atoms in a compound or mixture	
X_0	Radiation length	g cm^{-2}
—	$4\alpha r e^2 N_A/A$	(716.408 g cm^{-2})$^{-1}$ for $A = 1$ g mol^{-1}
E_c	Critical energy	MeV
E_s	Scale energy $\sqrt{4\pi/\alpha}\ m_e c^2$	21.2052 MeV
R_M	Molière radius	MeV g^{-1} cm^2

[a] For ρ in g cm^{-3}.

23.2. Ionization energy loss by heavy particles [1–5]

Moderately relativistic charged particles other than electrons lose energy in matter primarily by ionization. The mean rate of energy loss (or stopping power) is given by the Bethe-Bloch equation,

$$-\frac{dE}{dx} = Kz^2\frac{Z}{A}\frac{1}{\beta^2}\left[\frac{1}{2}\ln\frac{2m_ec^2\beta^2\gamma^2T_{\max}}{I^2} - \beta^2 - \frac{\delta}{2}\right] . \tag{23.1}$$

Here $T_{\max}$ is the maximum kinetic energy which can be imparted to a free electron in a single collision, and the other variables are defined in Table 23.1. The units are chosen so that dx is measured in mass per unit area, *e.g.*, in g cm^{-2}.

In this form, the Bethe-Bloch equation describes the energy loss of pions in a material such as copper to about 1% accuracy for energies between about 6 MeV and 6 GeV. At lower energies corrections for tightly-bound atomic electrons and other effects must be made, and at higher energies radiative effects begin to be important. These limits of validity depend on both the effective atomic number of the absorber and the mass of the slowing particle. Low-energy effects will be discussed in Sec. 23.2.2.

The function as computed for pions on copper is shown by the solid curve in Fig. 23.1, and for pions on other materials in Fig. 23.2. A minor dependence on M at the highest energies is introduced through $T_{\max}$, but for all practical purposes in high-energy physics dE/dx in a given material is a function only of β. Except in hydrogen, particles of the same velocity have very similar rates of energy loss in different materials; there is a slow decrease in the rate of energy loss with increasing Z. The qualitative difference in stopping power behavior at high energies between a gas (He) and the other materials shown in Fig. 23.2 is due to the density-effect correction, δ, discussed below. The stopping power functions are characterized by broad minima whose position drops from $\beta\gamma = 3.5$ to 3.0 as Z goes from 7 to 100.

In practical cases, most relativistic particles (*e.g.*, cosmic-ray muons) have energy loss rates close to the minimum, and are said to be minimum ionizing particles, or mip's.

Eq. (23.1) may be integrated to find the total range R for a particle which loses energy only through ionization. Since dE/dx depends only on β, R/M is a function of E/M or pc/M. In practice, range is a useful concept only for low-energy hadrons ($R \lesssim \lambda_I$, where λ_I is the nuclear interaction length), and for muons below a few hundred GeV (above which radiative effects dominate). R/M as a function of $\beta\gamma = pc/M$ is shown for a variety of materials in Fig. 23.3.

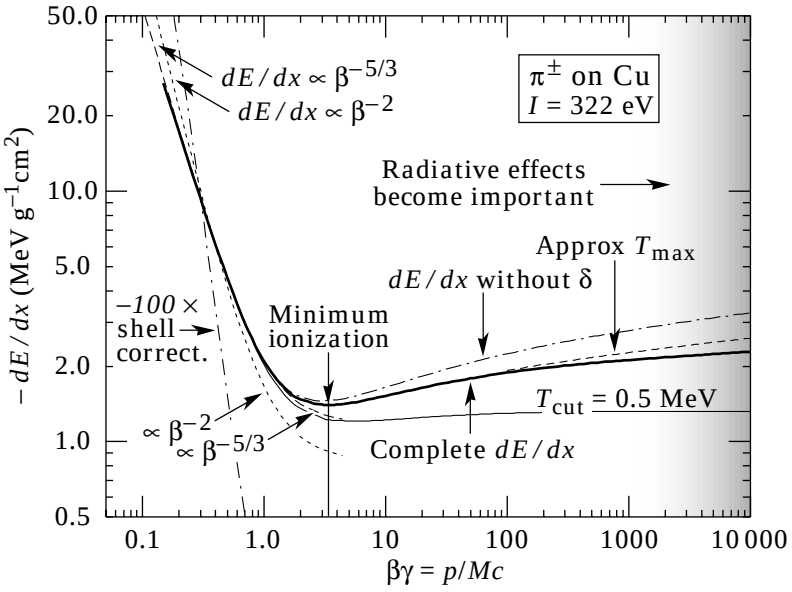

Figure 23.1: Energy loss rate in copper. The function without the density-effect correction, δ, is also shown, as is the loss rate excluding energy transfers with $T > 0.5$ MeV. The shell correction is indicated. The conventional β^{-2} low-energy approximation is compared with $\beta^{-5/3}$.

For a particle with mass M and momentum $M\beta\gamma c$, $T_{\max}$ is given by

$$T_{\max} = \frac{2m_e c^2 \beta^2\gamma^2}{1 + 2\gamma m_e/M + (m_e/M)^2} \ . \tag{23.2}$$

It is usual [1,2] to make the "low-energy" approximation $T_{\max} = 2m_e c^2 \beta^2\gamma^2$, valid for $2\gamma m_e/M \ll 1$; this, in fact, is done implicitly in many standard references. For a pion in copper, the error thus introduced into dE/dx is greater than 6% at 100 GeV. The correct expression should be used.

At energies of order 100 GeV, the maximum 4-momentum transfer to the electron can exceed 1 GeV/c, where structure effects significantly modify the cross sections. This problem has been investigated by J.D. Jackson [6], who concluded that for hadrons (but not for large nuclei) corrections to dE/dx are negligible below energies where radiative effects dominate. While the cross section for rare hard collisions is modified, the average stopping power, dominated by many softer collisions, is almost unchanged.

The mean excitation energy I is $(10 \pm 1$ eV$) \times Z$ for elements heavier than sulphur. The values adopted by the ICRU for the chemical elements [7] are now in wide use; these are shown in Fig. 23.4. Machine-readable versions can also be found [8]. Given the availability of these constants and their variation with atomic structure, there seems little point to depending upon approximate formulae, as was done in the past.

Ionization losses by electrons and positrons [7,9,10] are not discussed here. Above the critical energy, which is a few tens of MeV in most materials (see Fig. 23.7),

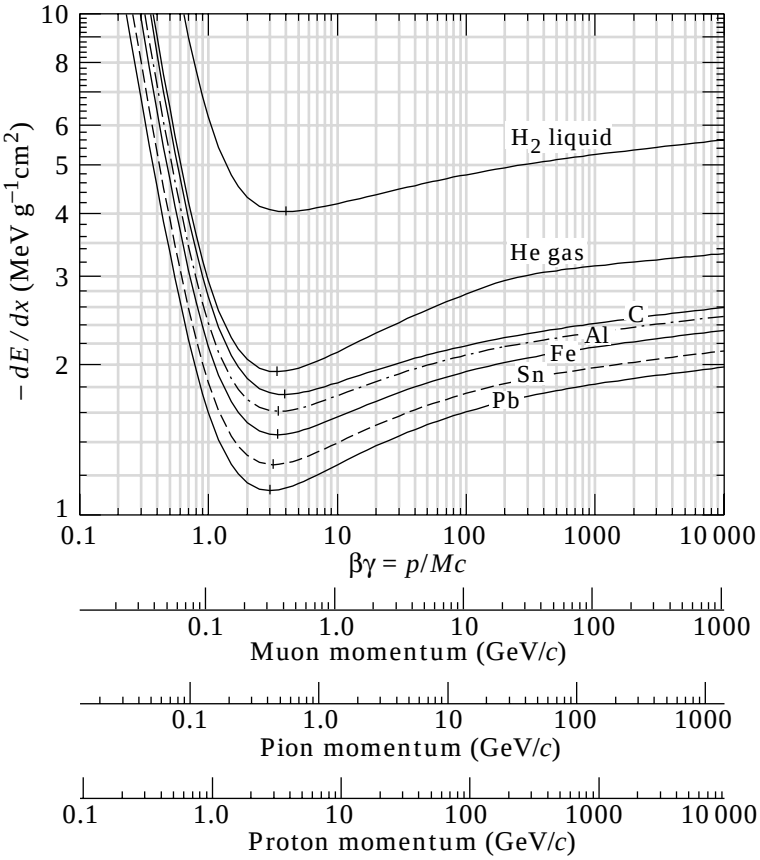

Figure 23.2: Energy loss rate in liquid (bubble chamber) hydrogen, gaseous helium, carbon, aluminum, tin, and lead.

bremsstrahlung is the dominant source of energy loss. This important case is discussed below. The contributions of various electron energy-loss processes in lead are shown in Fig. 24.4.

23.2.1. ***The density effect***: As the particle energy increases, its electric field flattens and extends, so that the distant-collision contribution to Eq. (23.1) increases as $\ln\beta\gamma$. However, real media become polarized, limiting the field extension and effectively truncating this part of the logarithmic rise [4,11–14]. At very high energies,

$$\delta/2 \to \ln(\hbar\omega_p/I) + \ln\beta\gamma - 1/2 \ , \tag{23.3}$$

where $\delta/2$ is the density effect correction introduced in Eq. (23.1) and $\hbar\omega_p$ is the plasma energy defined in Table 23.1. A comparison with Eq. (23.1) shows that $|dE/dx|$ then grows as $\ln\beta\gamma$ rather than $\ln\beta^2\gamma^2$, and that the mean excitation energy I is replaced by the plasma energy $\hbar\omega_p$. The stopping power as calculated with and without the density effect correction is shown in Fig. 23.1. Since the plasma frequency scales as the square

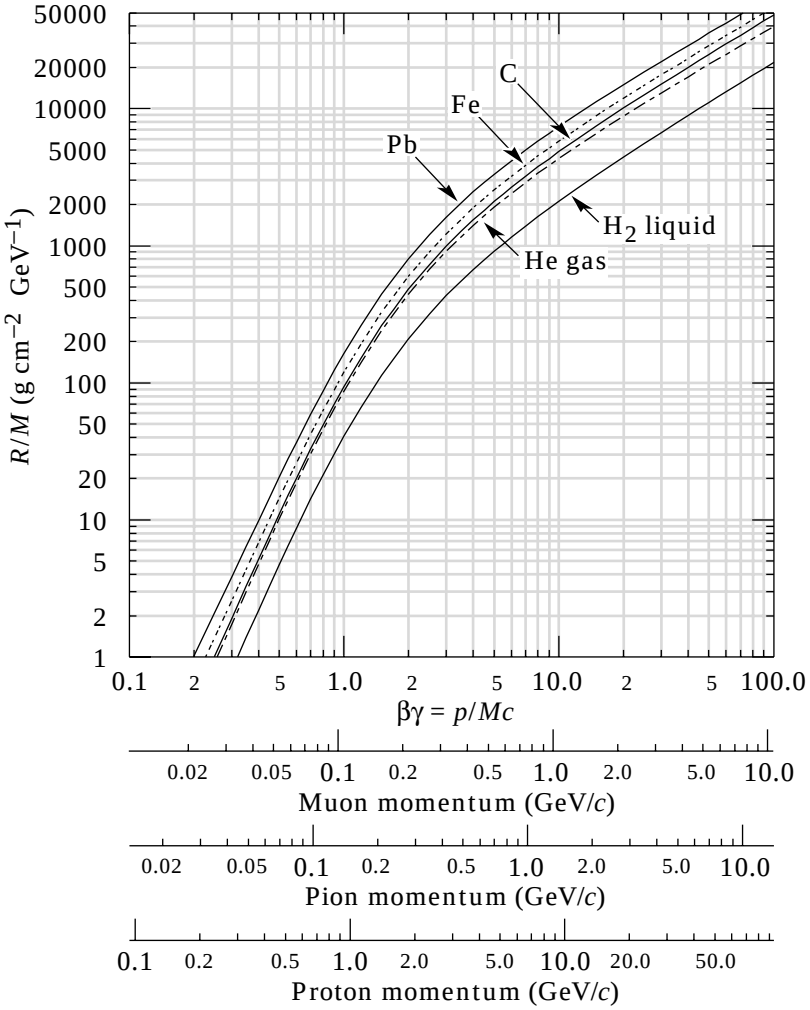

Figure 23.3: Range of heavy charged particles in liquid (bubble chamber) hydrogen, helium gas, carbon, iron, and lead. For example: For a K^+ whose momentum is 700 MeV/c, $\beta\gamma = 1.42$. For lead we read $R/M \approx 396$, and so the range is 195 g cm^{-2}.

root of the electron density, the correction is much larger for a liquid or solid than for a gas, as is illustrated by the examples in Fig. 23.2.

The density effect correction is usually computed using Sternheimer's parameterization [11]:

$$\delta = \begin{cases} 2(\ln 10)x - \overline{C} & \text{if } x \geq x_1; \\ 2(\ln 10)x - \overline{C} + a(x_1 - x)^k & \text{if } x_0 \leq x < x_1; \\ 0 & \text{if } x < x_0 \text{ (nonconductors);} \\ \delta_0 10^{2(x-x_0)} & \text{if } x < x_0 \text{ (conductors)} \end{cases} \tag{23.4}$$

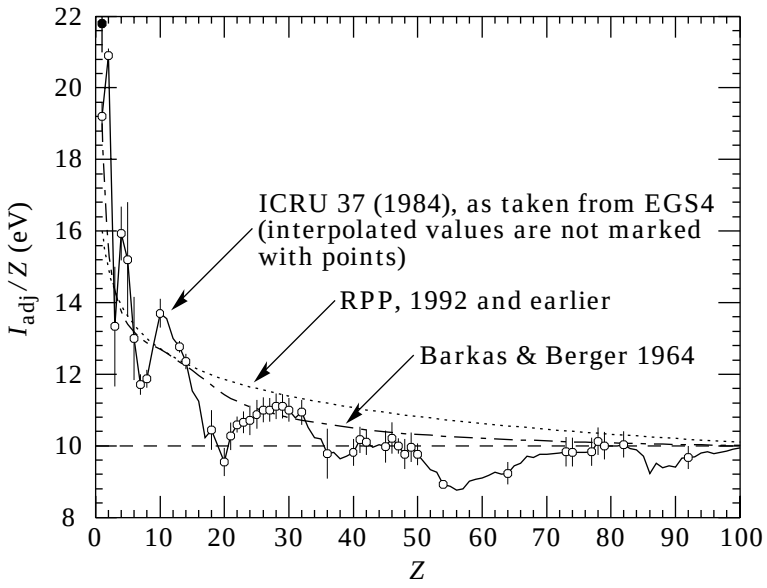

Figure 23.4: Excitation energies (divided by Z) as adopted by the ICRU [7]. Those based on measurement are shown by points with error flags; the interpolated values are simply joined. The solid point is for liquid H_2; the open point at 19.2 is for H_2 gas. Also shown are curves based on two approximate formulae.

Here $x = \log_{10}\eta = \log_{10}(p/Mc)$. $\overline{C}$ (the negative of the C used in Ref. 11) is obtained by equating the high-energy case of Eq. (23.4) with the limit given in Eq. (23.3). The other parameters are adjusted to give a best fit to the results of detailed calculations for momenta below $Mc\exp(x_1)$. Parameters for elements and nearly 200 compounds and mixtures of interest are published in a variety of places, notably in Ref. 14. A recipe for finding the coefficients for nontabulated materials given by Sternheimer and Peierls [13] is summarized in Ref. 10.

The remaining relativistic rise can be attributed to large energy transfers to a few electrons. If these escape or are otherwise accounted for separately, the energy deposited in an absorbing layer (in contrast to the energy lost by the particle) approaches a constant value, the Fermi plateau (see Sec. 23.2.5 below). The curve in Fig. 23.1 labeled "$T_{\rm cut} = 0.5$ MeV" illustrates this behavior. At extreme energies (*e.g.*, $>$ 321 GeV for muons in iron), radiative effects are more important than ionization losses. These are especially relevant for high-energy muons, as discussed in Sec. 23.6.

23.2.2. ***Energy loss at low energies***: A shell correction C/Z is often included in the square brackets of Eq. (23.1) [3,5,7] to correct for atomic binding having been neglected in calculating some of the contributions to Eq. (23.1). We show the Barkas form [3] in Fig. 23.1. For copper it contributes about 1% at $\beta\gamma = 0.3$ (kinetic energy 6 MeV for a pion), and the correction decreases very rapidly with energy.

Eq. (23.1) is based on a first-order Born approximation. Higher-order corrections, again important only at lower energy, are normally included by adding a term $z^2 L_2(\beta)$ inside the square brackets.

An additional "Barkas correction" $zL_1(\beta)$ makes the stopping power for a negative particle somewhat larger than for a positive particle with the same mass and velocity. In a 1956 paper, Barkas *et al.* noted that negative pions had a longer range than positive pions [15]. The effect has been measured for a number of negative/positive particle pairs, most recently for antiprotons at the CERN LEAR facility [16].

A detailed discussion of low-energy corrections to the Bethe formula is given in ICRU Report 49 [5]. When the corrections are properly included, the accuracy of the Bethe-Bloch treatment is accurate to about 1% down to $\beta \approx 0.05$, or about 1 MeV for protons.

For $0.01 < \beta < 0.05$, there is no satisfactory theory. For protons, one usually relies on the empirical fitting formulae developed by Andersen and Ziegler [5,17]. For particles moving more slowly than $\approx 0.01c$ (more or less the velocity of the outer atomic electrons), Lindhard has been quite successful in describing electronic stopping power, which is proportional to β [18,19]. Finally, we note that at low energies, *e.g.*, for protons of less than several hundred eV, non-ionizing nuclear recoil energy loss dominates the total energy loss [5,19,20].

As shown in ICRU49 [5] (using data taken from Ref. 17), the nuclear plus electronic proton stopping power in copper is 113 MeV $\mathrm{cm}^2\,\mathrm{g}^{-1}$ at $T = 10$ keV, rises to a maximum of 210 MeV $\mathrm{cm}^2\,\mathrm{g}^{-1}$ at 100–150 keV, then falls to 120 MeV $\mathrm{cm}^2\,\mathrm{g}^{-1}$ at 1 MeV. Above 0.5–1.0 MeV the corrected Bethe-Block theory is adequate.

23.2.3. ***Fluctuations in energy loss***: The quantity $(dE/dx)\delta x$ is the mean energy loss via interaction with electrons in a layer of the medium with thickness δx. For finite δx, there are fluctuations in the actual energy loss. The distribution is skewed toward high values (the Landau tail) [1,21]. Only for a thick layer [$(dE/dx)\delta x \gg T_{\mathrm{max}}$] is the distribution nearly Gaussian. The large fluctuations in the energy loss are due to the small number of collisions involving large energy transfers. The fluctuations are smaller for the so-called restricted energy loss rate, as discussed in Sec. 23.2.5 below.

23.2.4. ***Energy loss in mixtures and compounds***: A mixture or compound can be thought of as made up of thin layers of pure elements in the right proportion (Bragg additivity). In this case,

$$\frac{dE}{dx} = \sum w_j \left.\frac{dE}{dx}\right|_j , \tag{23.5}$$

where $dE/dx|_j$ is the mean rate of energy loss (in MeV g cm^{-2}) in the jth element. Eq. (23.1) can be inserted into Eq. (23.5) to find expressions for $\langle Z/A\rangle$, $\langle I\rangle$, and $\langle\delta\rangle$;

for example, $\langle Z/A\rangle = \sum w_j Z_j/A_j = \sum n_j Z_j / \sum n_j A_j$. However, $\langle I\rangle$ as defined this way is an underestimate, because in a compound electrons are more tightly bound than in the free elements, and $\langle\delta\rangle$ as calculated this way has little relevance, because it is the electron density which matters. If possible, one uses the tables given in Refs. 14 and 10, which include effective excitation energies and interpolation coefficients for calculating the density effect correction for the chemical elements and nearly 200 mixtures and compounds. If a compound or mixture is not found, then one uses the recipe for δ given in Ref. 13 (or Ref. 22), and calculates $\langle I\rangle$ according to the discussion in Ref. 9. (Note the "13%" rule!)

23.2.5. ***Restricted energy loss rates for relativistic ionizing particles***: Fluctuations in energy loss are due mainly to the production of a few high-energy knock-on electrons. Practical detectors often measure the energy *deposited*, not the energy *lost*. When energy is carried off by energetic knock-on electrons, it is more appropriate to consider the mean energy loss excluding energy transfers greater than some cutoff $T_{\rm cut}$. The restricted energy loss rate is

$$-\left.\frac{dE}{dx}\right|_{T<T_{\rm cut}} = Kz^2\frac{Z}{A}\frac{1}{\beta^2}\left[\frac{1}{2}\ln\frac{2m_ec^2\beta^2\gamma^2T_{\rm upper}}{I^2} - \frac{\beta^2}{2}\left(1+\frac{T_{\rm upper}}{T_{\rm max}}\right) - \frac{\delta}{2}\right] \tag{23.6}$$

where $T_{\rm upper} = {\rm MIN}(T_{\rm cut}, T_{\rm max})$. This form agrees with the equation given in previous editions of this *Review* [23] for $T_{\rm cut} \ll T_{\rm max}$ but smoothly joins the normal Bethe-Bloch function (Eq. (23.1)) for $T_{\rm cut} > T_{\rm max}$.

23.2.6. ***Energetic knock-on electrons (δ rays)***: The distribution of secondary electrons with kinetic energies $T \gg I$ is given by [1]

$$\frac{d^2N}{dTdx} = \frac{1}{2}Kz^2\frac{Z}{A}\frac{1}{\beta^2}\frac{F(T)}{T^2} \tag{23.7}$$

for $I \ll T \le T_{\rm max}$, where $T_{\rm max}$ is given by Eq. (23.2). The factor F is spin-dependent, but is about unity for $T \ll T_{\rm max}$. For spin-0 particles $F(T) = (1 - \beta^2 T/T_{\rm max})$; forms for spins 1/2 and 1 are also given by Rossi [1]. When Eq. (23.7) is integrated from $T_{\rm cut}$ to $T_{\rm max}$,one obtains the difference between Eq. (23.1) and Eq. (23.6). For incident electrons, the indistinguishability of projectile and target means that the range of T extends only to half the kinetic energy of the incident particle. Additional formulae are given in Ref. 24. Equation (23.7) is inaccurate for T close to I: for $2I \lesssim T \lesssim 10I$, the $1/T^2$ dependence above becomes approximately $T^{-\eta}$, with $3 \lesssim \eta \lesssim 5$ [25].

23.2.7. ***Ionization yields***: Physicists frequently relate total energy loss to the number of ion pairs produced near the particle's track. This relation becomes complicated for relativistic particles due to the wandering of energetic knock-on electrons whose ranges exceed the dimensions of the fiducial volume. For a qualitative appraisal of the nonlocality of energy deposition in various media by such modestly energetic knock-on electrons, see Ref. 26. The mean local energy dissipation per local ion pair produced, W, while essentially constant for relativistic particles, increases at slow particle speeds [27]. For gases, W can be surprisingly sensitive to trace amounts of various contaminants [27]. Furthermore, ionization yields in practical cases may be greatly influenced by such factors as subsequent recombination [28].